Eur. Phys. J. B **21**, 455–462 (2001)

THE EUROPEAN PHYSICAL JOURNAL B

EDP Sciences

Helix coil mixing in twist-storing polymers

S. Kutter and E.M. Terentjev[a]

Cavendish Laboratory, University of Cambridge, Madingley Road, Cambridge, CB3 0HE, UK

Received 16 November 2000 and Received in final form 6 February 2001

Abstract. Twist-storing polymers respond with elastic energy penalty to coherent or random twisting along the local chain axis away from its equilibrium, which can be straight (as in "ribbons") or helical (as in DNA and other biopolymers). Here we study the equilibrium conformation of such polymers, focusing on the thermodynamic balance between twist and writhe, resulting from the competition between the random coil entropy and the potential energy stored in superhelical portions of the polymer chain. Two macroscopic variables characterise such a chain, the end-to-end distance R and the link number Lk, which is a topological invariant of a given polymer with clamped ends. We find that with increasing link number Lk, the chain accommodates its excess twist in growing plectonemes, unless forced out of this state by stretching its end-to-end distance R. We calculate the force–extension relation, which exhibits crossovers between different deformation regimes.

PACS. 87.15.-v Biomolecules: structure and physical properties – 61.41.+e Polymers, elastomers, and plastics – 36.20.Ey Conformation (statistics and dynamics)

1 Introduction

Conformation and physical properties of biopolymers attract a high level of attention from a variety of classical physics fields. The motivation, apart from an appealing contact with life sciences, is that this class of polymers presents new challenges for theoretical and experimental physics. First, a large body of theoretical work provides a deep insight into the physical behaviour of single polymers and entangled and crosslinked polymer networks by applying statistical mechanics to simple mechanical polymer models, reflecting some key features of a system and neglecting a large number of irrelevant complexities. Secondly, recent advances in experimental techniques made it possible to observe single molecules, in particular DNA and polypeptides, and to measure their individual mechanical properties [1–3]. Thirdly, experimental as well as theoretical physics of biopolymers, as well as of other twist-storing line objects, provides a playground for topology and knot theory.

There are a variety of different models to explain the physical behaviour of long chain polymers, starting from the simplest random walk, where the polymer path is modelled by a sequence of uncorrelated steps in space (see [4] for key examples). For polymers of simple chemical structure or for very long chains, this model is appropriate, providing an adequate description of basic properties. More complex polymers exhibit a certain bending stiffness that preserves the direction of the polymer over a persistence length A. This leads to the classical model of inextensible semiflexible polymer or worm-like chain [5–8]. Many investigations have been carried out on this model, but we will refer later to the recent work of Thirumalai *et al.* [9], which provides a closed expression for the free energy of a worm-like chain spanning the full range of end-to-end distance R variation. The worm-like chain model is, again, well adapted to only a certain class of polymers. For instance, it assumes that the stiffness of the chain is equally strong in all directions. Ribbon or sheet-like polymers, however, are easy to bend in one direction, but hard to deform in the perpendicular direction (see *e.g.* [10]). To avoid additional complications, we restrict ourselves in this article only to polymers with an isotropic chain cross section having a single persistence length A.

The models mentioned so far describe a polymer as an essentially one-dimensional line with, perhaps, isotropic or anisotropic bending modulus. But many polymers, as for example DNA and polypeptides, can resist an external torque and change their local and global configuration on imposed twisting, *i.e.* on rotation of one chain end around its central axis, while the other end is fixed. Such polymer chains are called twist-storing, in contrast to more simple systems that could freely unwind the twist. One can visualise this behaviour by twisting a rope or a rubber tube and observing the appearance of double-helical, interwound structures, called plectonemes, see Figure 1. The most familiar example is, of course, the telephone cord forming interwound helices as the receiver is rotated and placed back on the phone. These structures and their stability have been investigated within the framework of

[a] e-mail: emt1000@cam.ac.uk

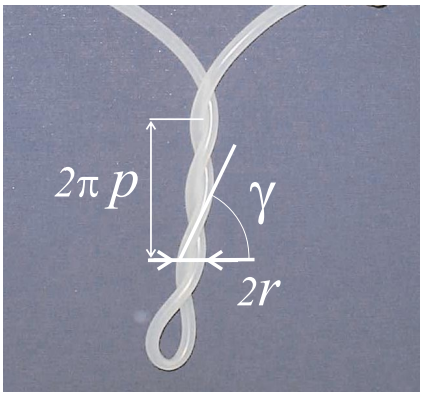

Fig. 1. A macroscopic plectoneme formed by a twisted rubber tube. The image also defines the parameters used in the theory: the plectoneme radius r, the pitch rate p and the angle γ, which the winding strands make with the plectoneme axis.

solid mechanics and elasticity theory, see for example the most recent work reported in [11–14].

Experiments on single DNA molecules have recently received a lot of attention [1–3,15] and prompted theoretical work on the behaviour of twist-storing DNA [16–18]. Some of this work deals with particular features of DNA, like denaturated states, characterised by separation of the two linear strands that make up the famous DNA double helix. In this article, we develop a mechanical model that applies to polypeptides and DNA, but also describes a wider class of semiflexible polymers with an added local twist rigidity. We combine the classical polymer statistical mechanics [9] with mean field arguments similar to the method used by Marko [16], and refer to the topological theory of link number illustrated by Fuller [19]. Our work is inspired by the work of Marko and Siggia [16,17] and arrives at similar results and conclusions. Their investigations focus on the behaviour of DNA superstructure by calculating the balance of segments accommodated in solenoidal and plectonemic segments. In contrast to their work, our model is an investigation on a more basic level: the competition between elastic effects favouring plectonemes and entropic free energy favouring random walk configurations. Our results for the force-extension relation are also very close to the numerical study [14], where the Fixman-Kovak model of random coil [8] has been employed.

This article describes the model of a twist-storing polymer chain that finds an equilibrium between the enthalpic plectoneme regions and entropy-dominated worm-like random coil portions. Section 2 gives the general solution scheme. Numerical results and the interpretation for the case of a single twist-storing chain are given in Section 3, where we also discuss limiting cases and analytical expressions for the mechanical response in certain characteristic regimes of deformation.

2 Model

In classical polymer theories, as the random walk model or the Gaussian chain approximation [4], the path traced by the chain in space is analogous to a diffusive process in time. The directions of two adjacent segments are not correlated in these simple models. One can derive simple diffusion laws like $\langle R^2 \rangle \propto L$, where R is the end-to-end distance and L the total arc length of the polymer, or $F \propto R^2$, where F is the chain free energy at a fixed R. In a more realistic approach, addressing polymers with an internal bending rigidity of their bonds, one introduces a persistence or correlation length, A, over which the polymer preserves its direction [6–8] (inelastic semiflexible polymer, or worm-like chain). This is equivalent to introducing an energy penalty associated with any deformation away from the zero-temperature ground state, which is a straight line in this case. The elastic bending energy of a polymer of length L and arc length parametrisation s can be written as:

$$\beta H_\mathrm{b} = \int_0^L \frac{A}{2}\kappa^2(s)\mathrm{d}s = \int_0^L \frac{A}{2}\left|\frac{\partial^2 \mathbf{r}}{\partial s^2}\right|^2 \mathrm{d}s, \qquad (1)$$

where $\kappa(s)$ is the local curvature of the path $\mathbf{r}(s)$ and $\beta = 1/k_\mathrm{B}T$ with k_B the Boltzmann constant and T the temperature. This model can be further generalised to account for anisotropy of the bending energy (the case of "ribbons" and "belts", see for example [10]). Here we restrict ourselves to the uniaxial case, assuming the chain is equally rigid in response to bending in any direction away from its local tangent vector $\mathbf{t}(s) = \partial\mathbf{r}/\partial s$, $\mathbf{t}^2(s) = 1$. In making this assumption which is clearly inadequate for flat ribbon-like polypeptides, we have in mind a more common coarse-grained case of biopolymers, tightly twisted in the secondary structure – or telephone cords. In such cases, when the pitch of chain twisting about its local tangent is smaller than the persistence length A, one may assume the effective bending constant averaged over this helical pitch and, thus, losing its anisotropy. In case of DNA, this is justified by comparing the helical repeat distance of about 3.5 nm with the bending stiffness of about 50 nm [3,16].

We then introduce an additional twist stiffness, that resists a local torque applied parallel to the polymer central axis $\mathbf{t}(s)$. Our initial simplified model is therefore described by the following Hamiltonian:

$$\beta H \equiv \beta H_\mathrm{b} + \beta H_\mathrm{tw} = \int_0^L \left(\frac{A}{2}\kappa^2(s) + \frac{C}{2}\omega^2(s)\right)\mathrm{d}s, \quad (2)$$

where $\omega(s)$ is the local twist rate, A and C are the persistence lengths for the chain bending and twisting degrees of freedom, respectively. The macroscopic analogue of our model would be an elastic tube of circular cross-section or a semiflexible cylinder with a line drawn on the side to keep track of the internal twisting degree of freedom, *cf.* Figure 1. The model represented by equation (2) is oversimplified. In addition to the bending anisotropy, it does not take into account the twist-bend coupling terms,

which have attracted attention and brought some interesting new results recently [20,21]. All such omitted terms, although having an effect on the chain conformation and dynamics, do not change the essential physics of free energy balance between twist and bend. We, therefore, restrict the microscopic polymer description to the minimal model (2).

2.1 Link, twist and writhe

By including the twist stiffness, the model polymer can respond to externally applied torques. If the two ends of the chain are clamped in order that they can neither move in space nor rotate, the conserved quantity, besides the constrained end-to-end distance R, is the link number Lk [13]. The link number Lk is uniquely defined for a closed loop. Consider for example an elastic tube with a line drawn on the side closed into a loop. Both the central axis of the tube and the line on the side are closed paths in space, which in general cannot be disentangled. The link number gives the number of crossings that are necessary to separate these two loops. For open segments, one can still define a link number provided the two ends can neither move in space nor rotate around their axis. One joins the two ends by an imaginary fixed curve (*e.g.* a straight line) and defines the link number of the open segment as the link number of the total closed loop made up of the open segment plus the closure [13], see also [22]. The link number defined in this way depends on the the choice of the imaginary closure. Deformations of the open polymer segment conserve the link number, provided that the end points of the open segment are clamped and the open segment never crosses the closing curve during deformation.

For closed loops and for open segments with clamped ends, the link number is related to the internal twist Tw and the writhe Wr [19,23,24]:

$$Lk = Tw + Wr, \tag{3}$$

where $Tw = \frac{1}{2\pi}\oint \omega(s)\mathrm{d}s$ is the total twist and Wr the writhe of the curve. The writhe is a number solely determined by the trajectory of the chain (or tube) axis $\mathbf{r} = \mathbf{r}(s)$ and independent of the internal twist $\omega(s)$. In case of the open segment, the two end points should be joined by a twistless segment, and Tw is given by a linear integral along the chain: $Tw = \frac{1}{2\pi}\int \omega(s)\mathrm{d}s$.

2.2 Helix vs. coil

Macroscopically, one can observe that a twisted rope forms localised double-helical structures, the plectonemes, as one increases the effective link number by rotating one end around its central axis, keeping the other end fixed. We expect a similar behaviour for microscopic systems, although in this case the highly localised plectonemes stand in competition with thermal fluctuations and chain configurational entropy. The polymer will accommodate some of its length in plectonemic superhelices, whereas the remaining part will be in a "disordered" coil state, similar to a random walk of an ordinary polymer chain. Due to thermal fluctuations, the contribution of the random coil portions to the total writhe Wr can be set to zero statistically, since, for example, the coil segments have statistically equal access to states that are mirror images of each other, which have writhe of opposite sign. In contrast, the coherently bent plectonemic segments will significantly contribute to the writhe Wr. In a saddle point approximation, the plectonemic segments all wind with the same constant pitch rate p and radius r, defined in Figure 1.

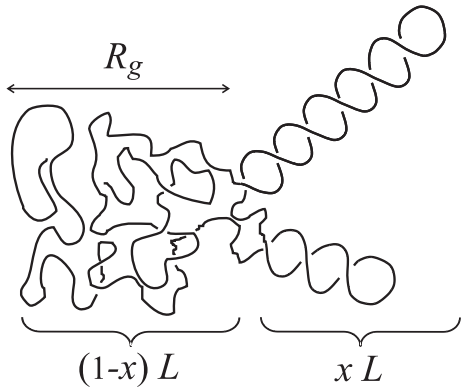

Fig. 2. A schematic view of the model showing the random coil part (with a radius of gyration R_g proportional to the end-to-end distance R) and two plectonemes. The model does not account for the edge effects of plectonemes and thus for the number of separate plectonemic superhelices. Hence conformations with different numbers of plectonemes may all be represented by a conformation with only one plectoneme absorbing the same total arc length portion xL.

We are left with the following contributions to the total link number Lk (note that Lk is generally not an additive quantity that can be summed up over different chain segments; here, we adopt an approximation):

$$Lk = \frac{1}{2\pi}\int_0^L \omega(s)\mathrm{d}s + Wr_\mathrm{p}, \tag{4}$$

where $Wr_\mathrm{p} = 2N\sin\gamma = 2N\frac{p}{\sqrt{p^2+r^2}}$ is the writhe of a plectoneme, consisting of N full turns with pitch rate p, pitch angle γ and winding radius r.

The winding radius of the plectoneme is determined by short range forces acting between the two strands in contact. Here we treat the radius of the plectoneme as a known fixed parameter of the model, since we do not deal with any interactions between distant segments. We assume that the plectonemic portions of the polymer chain take up a total fraction x of the polymer arc length, Figure 2. In this sense, the model does not account for the number of separated plectonemes, assuming they all contribute additively to the potential energy. Then the number of turns N in all plectonemic segments is given by:

$$N = \frac{xL}{4\pi\sqrt{p^2+r^2}}\cdot \tag{5}$$

The following partition function describes the system with constrained end-to-end distance R and link number Lk:

$$Z \equiv \mathrm{e}^{-\beta F(R,Lk)} = \sum_{\text{states } i} \mathrm{e}^{-\beta H[i]} \delta(R - R[i])\ \delta(Lk - Lk[i]). \tag{6}$$

The simplified Hamiltonian in equation (2) decouples bending and twisting energies. Moreover, the bending energy βH_b resolves into two separate contributions: elastic energy of the plectonemic fraction and the random walk fraction:

$$\beta H_\mathrm{b} = \beta H_\mathrm{rw} + \beta H_\mathrm{pl}, \tag{7}$$

with

$$\beta H_\mathrm{pl} = xL \left(\frac{A}{2} \frac{r^2}{(r^2+p^2)^2} \right). \tag{8}$$

For a given spatial path, the polymer will fluctuate around a state that minimises the twist energy

$$\beta H_\mathrm{tw} = \int_0^L \frac{C}{2} \omega^2(s) \mathrm{d}s, \tag{9}$$

which is given by $\omega(s) = \omega = \text{const}$. Therefore, in case of the saddle point approximation $\omega = \text{const.}$, the topological constraint (4) simplifies to:

$$Lk = \frac{L}{2\pi}\omega + \frac{xLp}{2\pi(p^2+r^2)} \cdot \tag{10}$$

As a result of these considerations, we obtain the statistical weight $Z(R, Lk)$ as a sum over three microscopic variables, the plectonemic fraction x, the twist rate ω and the pitch rate of the plectoneme ω.

$$Z(R,Lk) = \sum_{x,\omega,p} \mathrm{e}^{-\beta H_\mathrm{tw}} \mathrm{e}^{-\beta H_\mathrm{pl}} \delta(Lk - Lk(x,\omega,p)) \mathrm{e}^{-\beta F(R,x)} \tag{11}$$

where $\mathrm{e}^{-\beta F(R,x)}$ is the partial statistical weight of the polymer segment of length $(1-x)L$ that is accommodated in the random walk portion of the chain, see Figure 2.

In our simplified picture neglecting the end effects, the plectonemes cannot contribute to the end-to-end distance R. Hence, the random coil portion of the chain spans all of the constrained end-to-end distance R. The corresponding statistical weight $\mathrm{e}^{-\beta F(R,x)}$ is formally given by a path integral, for which Thirumalai *et al.* [9] have obtained a closed solution:

$$\begin{aligned} \mathrm{e}^{-\beta F(R,x)} &= \int \mathcal{D}[\mathbf{t}(s)] \mathrm{e}^{-\int \frac{A}{2}(\frac{\partial \mathbf{t}}{\partial s})^2 \mathrm{d}s} \delta\left(\mathbf{R} - \int \mathbf{t}\ \mathrm{d}s \right) \\ &\approx M(x) \frac{1}{(1-\rho^2)^{9/2}} \exp\left(-\frac{9(1-x)L}{8A(1-\rho^2)} \right) \end{aligned} \tag{12}$$

where the integrals running over the polymer length s are taken over the fraction of chain that is accommodated in the random walk segment, *i.e.* from 0 to $(1-x)L$. The resulting expression (12) for the statistical weight includes the normalisation factor, given by

$$M(x) = \frac{4\alpha^{7/2}\mathrm{e}^\alpha}{\pi^{3/2}(4\alpha^2+12\alpha+15)}, \quad \text{with} \quad \alpha = \frac{9}{8}\frac{(1-x)L}{A},$$
$$\text{and} \quad \rho = \frac{R}{(1-x)L}\,.$$

Note that the normalisation constant $M(x)$ cannot be neglected in the main equation (11), as it is often the case in ordinary studies of semiflexible polymers. This constant is proportional to the conformation space available to the random walk segment of length $(1-x)L$, and, therefore, it contributes to the free energy balance between the competing plectonemic superhelical portion x and the disordered chain portion $(1-x)$. If, for example, most of the polymer forms a plectoneme, so $x \approx 1$, the normalisation constant N decreases dramatically, reflecting the loss of entropy due to the confinement of most of the polymer in the plectoneme.

After collecting all relevant terms and discarding unimportant constants, one obtains the following microscopic effective Hamiltonian contributing to the Gibbs sum in (11):

$$\begin{aligned} &\beta H_\mathrm{eff}(R, Lk; x, p) = \\ &xL\frac{A}{2}\frac{r^2}{(r^2+p^2)^2} + L\frac{C}{2}\omega^2 + \frac{9}{2}\log(1-\rho^2) \\ &+\frac{9}{8}\frac{(1-x)L}{A}\frac{1}{1-\rho^2} - \frac{3}{2}\log(1-x) \\ &+\frac{9}{8}\frac{L}{A}x + \log\left(4 + \frac{12}{\alpha} + \frac{15}{\alpha^2}\right) \end{aligned} \tag{13}$$

where the constraint equation (4) implies:

$$\omega = \frac{2\pi Lk}{L} - \frac{px}{p^2+r^2}\,. \tag{14}$$

In a saddle-point approximation, the true free energy is approximated by the minimum of the equation (13) given by the conditions $\partial H_\mathrm{eff}/\partial p = 0$ and $\partial H_\mathrm{eff}/\partial x = 0$:

$$\beta F(R, Lk) = \min_{x,p}(\beta H_\mathrm{eff}(R, Lk; x, p)). \tag{15}$$

3 Results and discussion

Throughout this section, when numerical results will be presented, we will use the following values of chain parameters, that can be found in the literature [3,16]: bending constant $A = 50$ nm, twist constant $C = 75$ nm. Furthermore, to be specific, we take the length of the polymer to be $L = 1000$ nm and the hard core winding radius of plectonemes to be $r = 1$ nm.

In the evaluation, we are left with two microscopic variables, the helical pitch rate p and the plectonemic fraction x; both variables are integrated out by saddle point approximation. The condition $\partial H_\mathrm{eff}/\partial p = 0$ yields a quartic

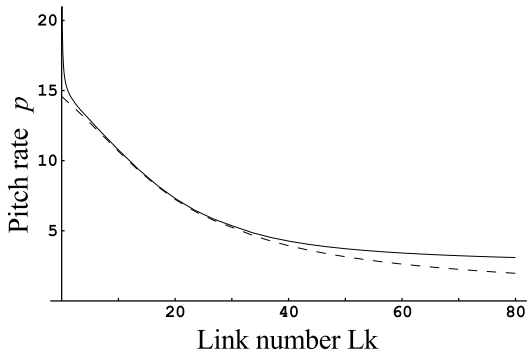

Fig. 3. Consistency check for the approximate solution for p given by equation (17) where the end-to-end distance was $R = 0$ and the link number $Lk = 10$. The full line is the exact numerical solution of equation (16) and the dashed one is the approximation (17).

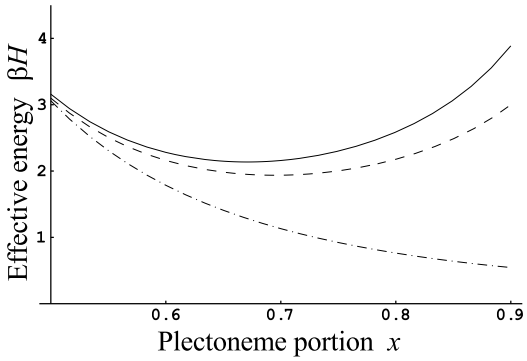

Fig. 4. Comparison of the full Hamiltonian βH^* in equation (18) (full line), the simplified form $\beta H_{\rm app}$ in equation (19) (dashed line) and the effect of omitting the 3rd term in equation (19), *i.e.* $\beta H_{\rm app} + 3/2 \log(1-x)$. The end-to-end distance and the link number are taken to be $R = 10$ and $Lk = 10$.

equation for p:

$$2\pi Lk\, Cp^4 - xL\, Cp^3 + r^2 xL\, Cp - 2r^2 L\, Ap - 2\pi r^4 Lk\, C = 0. \quad (16)$$

Assuming that the hard core radius of the polymer r is small compared to all other length scales, we only respect the two terms of the highest order in p and can solve the remaining equation trivially:

$$p = \frac{xL}{2\pi Lk}\,. \quad (17)$$

Although we have looked at the dominant contributions in the case of small r, in making the approximation (17) we have neglected some terms containing the dependency on x. One needs to check whether the approximation leading to (17) is valid. For this purpose, we will later perform a check for self-consistency.

The approximation (17) for the plectonemic pitch rate p yields the following effective Hamiltonian, now only depending on x:

$$\begin{aligned}\beta H^* = {} & \frac{9R^2}{16AL(1+R/L-x)} + \frac{9R^2}{16AL(1-R/L-x)} \\ & + \frac{(2\pi Lk)^4 r^2 [(2\pi Lk)^2 Cr^2 + AL^2 x]}{2L((2\pi Lk)^2 r^2 + L^2 x^2)^2} \\ & + \frac{9}{2}\log\left(1 - \left(\frac{R}{L(1-x)}\right)^2\right) - \frac{3}{2}\log(1-x) \\ & + \log\left(1 + \frac{80A^2}{27L^2(1-x)^2} + \frac{8A}{3L(1-x)}\right). \quad (18)\end{aligned}$$

Now the check for self-consistency of the approximation for p made in equation (17) is to numerically calculate the minimising value x^* for equation (18) and, by inserting x^*, to compare the exact numerical solution of equation (16) with the approximate solution (17) (see Fig. 3).

We observe that, except for very low link numbers Lk, the approximation is good. The divergence in p at low Lk describes a conformation when the polymer forms a plectoneme of divergent helical pitch rate p, which in this limit transforms into two parallel lines. However, the mismatch between the numerical solution of equation (16) and the approximation (17) at low link number does not cause further problems in energy calculations, since the plectonemic fraction x approaches 0 and thus reduces the energy stored in the plectonemic fraction to zero as well. The divergence in p, which is neglected by the approximation (17), only enhances this effect.

The function $\beta H^*(x)$ is divergent at $x = 1 - R/L$, due to the 2nd term, reflecting the high free energy penalty (due to entropy loss) as the two end points of the polymer are joined by straight paths, while the remaining polymer segment is entirely accommodated in a plectoneme. The formation of the plectoneme is favoured by the 3rd term which, on its own, would favour the maximal allowed $x \to 1$. However, the 5th term of expression (18) with its weak logarithmic divergence at $x = 1$ opposes this trend and contributes significantly to the location of the non-trivial minimum, in particular at small R: the divergence of the 2nd term, although stronger in the limiting case of an extended chain, is too weak and the early onset of the logarithmic divergence of the 5th term is essential (see Fig. 4).

Although all five terms are relevant to determine the exact location of the minimum, only three of them, namely the 2nd, the simplified 3rd and the 5th terms, capture the essential physical behaviour. We simplify the three remaining terms further and obtain:

$$\begin{aligned}\beta H_{\rm app} = {} & \frac{9R^2}{16AL(1-R/L-x)} \\ & + \frac{1}{2}(2\pi Lk)^4 \frac{Ar^2}{(xL)^3} - \frac{3}{2}\log(1-x). \quad (19)\end{aligned}$$

This approximation is valid at low link number, *i.e.* for $Lk \ll \frac{1}{2\pi}(L/r)$ and $Lk \ll \frac{1}{2\pi}\sqrt{A/C}(L/r)$, and this seems to be a very safe limit for long polymer chains. Note that this approximation eliminates the dependency on the twist constant C and the hard core radius r altogether,

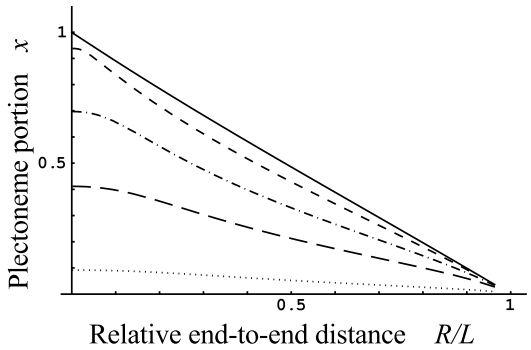

Fig. 5. The plectonemic fraction x against the end-to-end distance $R^* = (R/L)$ for different link number $Lk = 50$, 20, 10, 5 and 1 (running from the full to the dotted line).

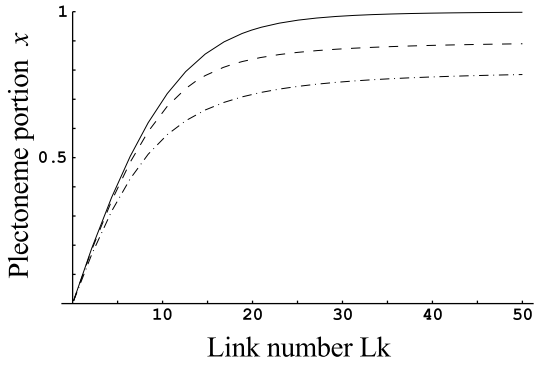

Fig. 6. The plectonemic fraction x against the link number Lk at a fixed end-to-end distance $R^* = 0$, 0.1, 0.2 (running from the full to the dash-dotted line); note how the plectonemic fraction is reduced by stretching the chain ends.

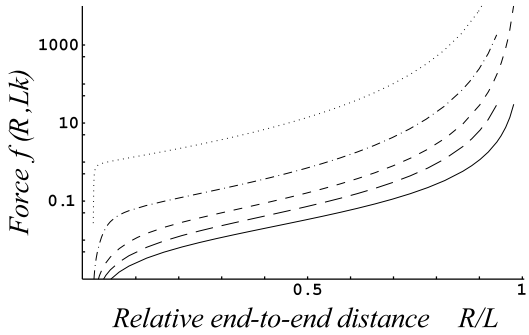

Fig. 7. The force $f(R, Lk)$ *vs.* the end-to-end distance R for different link number $Lk = 0$, 5, 10, 20, 50 (running from the full to the dotted line). The logarithmic scale of force allows fitting all curves on the same plot, over the full range of R/L variation.

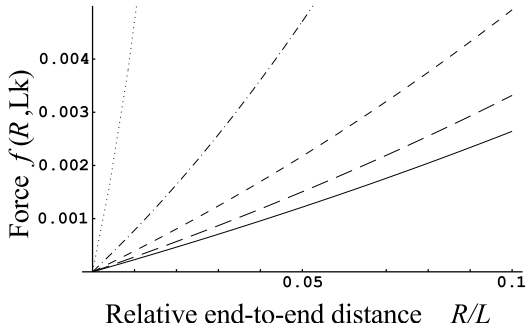

Fig. 8. Force f *vs.* end-to-end distance $R^* = \frac{R}{L}$ at very small R^*, at $Lk = 0$, 2, 5, 10 and 20 (running from the full to the dotted line).

reflecting the fact that the key competing factors are the entropy of the random coil and the elastic bending energy of the helical plectonemic portion of the polymer.

3.1 Free energy F(R, Lk)

From the simplified Hamiltonian (19), we can obtain numerical results for the plectonemic fraction x^* depending on the end-to-end distance R and the link number Lk. In Figure 5, we plot the plectonemic fraction x against the end-to-end distance at various link numbers Lk. We observe that on increasing the end-to-end distance R the plectonemic fraction decreases as the superhelix is forced to unwind. Also at low link number, the plectonemic fraction x is small reflecting the fact that the gain in mechanical energy by forming a plectoneme is lower than the corresponding entropy penalty; hence most of the polymer is accommodated in the random coil. Figure 6 shows the dependence of the plectonemic fraction x on the link number. At high link number, x saturates from below at the maximally allowed value $1-R/L$.

By inserting the saddle point value x^* back into the Hamiltonian $H_{\rm app}$ (19), we obtain an effective free energy $\beta F(R, Lk)$. Differentiating this energy βF with respect to R yields the force $f(R, Lk)$ acting between the end points of the polymer. This force is plotted in Figure 7 for various values of link number Lk. This result is very close to experimental data of [1–3], which has also been highlighted in the work of [14,17]. We observe the following behaviour:

- At low link number, the force is linear in the end-to-end distance R at low R, as expected from classical entropic polymer models. However, the effective spring constant depends on the link number: the polymer becomes tougher to stretch as the link number is increased. Figure 8 shows this by zooming on the region of very small R/L.
- At a link number of about 30, one can start observing three distinct regimes of the force: a linear extension regime at low R, as before at low Lk, a hardening of the polymer and finally an almost constant force plateau before the onset of the final divergence at $R = L$ (Figs. 7 and 9).
- We observe in Figure 5 that the plectonemic fraction x does not depend on R at very low R to the first approximation (the curves approach the vertical axis as $x \approx a - bR^2$, confirmed by series expansion of Eq. (19)). This regime is fairly extended at low link number (see dotted line in Fig. 5), but is reduced dramatically as link number is increased in such a way that it is not visible on the scale of Figure 5. This regime of

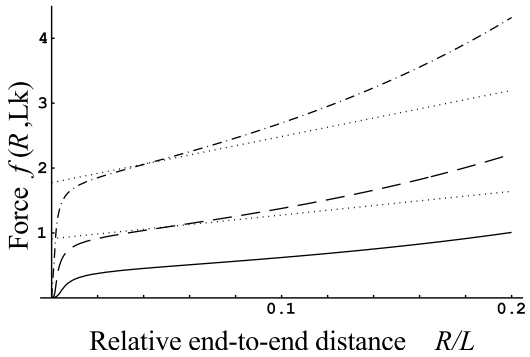

Fig. 9. Force f *vs.* end-to-end distance $R^* = \frac{R}{L}$ at high link number, *i.e.* $Lk = 40$, 50, 60 for the full, dashed and dash-dotted curve respectively. Straight dotted lines represent the corresponding asymptotic expressions in the plateau force regime (III), equation (22). Note that at very small R (regimes I or II), the force is linear in R, as shown in Figure 8, although this region is not visible here.

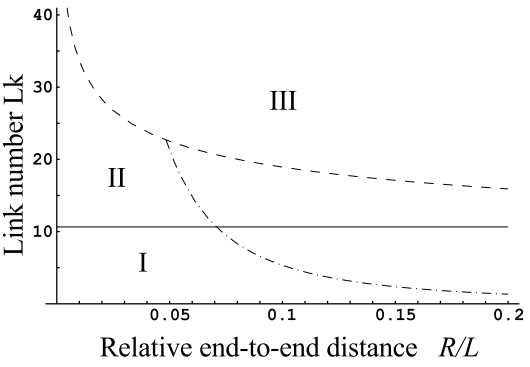

Fig. 10. Different regions of chain parameters where approximate expressions for the force $f(R, Lk)$ have been found. The full line is at $Lk = Lk^*$ and the dashed line follows $Lk = Lk^*\,(L/R)^{1/4}$. The dash-dotted "phase border" $Lk \ll \frac{1}{2}Lk^*(L/R)^2$ limits the regions I and II, where the plectonemic fraction x can be taken as independent of R, and the extension force is Hookean.

$x \approx$ const.(Lk) is related to the region where the force is linear in R (Fig. 9). As the link number is increased, the regime where the force is linear in R decreases to the same extent.

Approximate expressions for various characteristic regimes can be obtained using simple perturbation techniques. We will frequently use the following non-dimensional parameter, which will outline boundaries between the asymptotic regimes:

$$Lk^* = \frac{1}{2\pi}\left(\frac{L^3}{Ar^2}\right)^{1/4}.$$

For the particular choice of chain characteristics adopted in plotting the results, this number is $Lk^* \approx 10$. The different regions of parameters are shown diagrammatically in the "phase diagram" Figure 10.

3.2 Low link number Lk, small end-to-end distance R(I)

In a first approximation, the plectonemic fraction x does not depend on R at low R values (see dotted curve in Fig. 5), if $Lk \ll \frac{1}{2}Lk^*(L/R)^2$. However it depends linearly on the link number Lk (see full curve in Fig. 6). Hence the saddle point value of x satisfies the equation

$$\frac{\partial \beta H_{\rm app}}{\partial x}|_{R=0} = 0\,, \quad \text{or} \quad x^4 - d\,x + d = 0$$
$$\text{with} \quad d = (2\pi Lk)^4\frac{Ar^2}{L^3} = \left(\frac{Lk}{Lk^*}\right)^4,$$

giving $x \approx 2\pi Lk\left(r^2A/L^3\right)^{1/4} = Lk/Lk^*$ at small link number, *i.e.* for $Lk \ll Lk^*$, and small end-to-end distance, *i.e.* $R/L \ll 1$ and $R/L \ll \sqrt{Lk^*/2Lk}$.

Inserting this result into $\beta H_{\rm app}$ (19) and expanding for low R, we obtain for the force:

$$f = \frac{9}{8\beta}\frac{R}{AL}\frac{1}{1 - Lk/Lk^*}, \tag{20}$$

a "classical" Hookean expression with the spring constant modified by the link number.

3.3 High link number Lk, small end-to-end distance R(II)

As the discussion in previous sections reveals, the region of linear force is very small, reflecting the fact that the regime where x is independent of R at high Lk, is very small too (not visible in Fig. 5, but a more detailed plot would show it clearly). In this regime and at high link number, $Lk \gg Lk^*$, the plectonemic fraction x can be approximated by a constant value

$$x = 1 - \left(\frac{Lk^*}{Lk}\right)^4,$$

provided that $R/L \ll (Lk^*/Lk)^4$. After an evaluation procedure, similar to the previous case, one obtains the following expression for the force:

$$f = \left(\frac{Lk}{Lk^*}\right)^4\frac{9}{8\beta}\frac{R}{AL}\,. \tag{21}$$

In this case, the linear Hookean force is dominated by the high link number stored in the chain.

3.4 High link number Lk, intermediate R(III)

To find an approximate expression of the plateau regime as shown in Figure 9, we can approximate the plectonemic fraction x at non-infinitesimal R/L by a linear decrease

$$x = 1 - \frac{R}{L} - \sqrt{\frac{3}{8}}\frac{1}{(2\pi Lk)^2}\frac{LR}{Ar},$$

which is valid provided that $Lk \gg Lk^*$, $A \ll L$ and

$$\left(\frac{Lk^*}{Lk}\right)^4 \ll \frac{R}{L} \ll 1.$$

One finds the following expression for the force:

$$f = \frac{3}{2\beta}\left(\frac{Lk}{Lk^*}\right)^2 \frac{1}{L}\left[\left(\frac{Lk}{Lk^*}\right)^2 + \frac{\sqrt{6}}{2}\sqrt{\frac{L}{A}}\right]\left(1+4\frac{R}{L}\right)$$
$$\approx \frac{3}{2\beta}\left(\frac{Lk}{Lk^*}\right)^4 \frac{1}{L}\left(1+4\frac{R}{L}\right) \text{ for } Lk \gg \frac{1}{2\pi}\frac{L}{\sqrt{Ar}} \cdot \quad (22)$$

4 Conclusion

In this article, we have shown theoretical evidence for the formation of double-helical plectonemic structures in a twist-storing polymer due to the competition of elastic energy and entropic free energy. This effect leads to a novel macroscopic force-extension behaviour, for which we have found closed analytical expressions in important limiting cases.

S.K. gratefully enjoys support from an Overseas Research Scholarship, from the Cambridge Overseas Trust and from Corpus Christi College.

References

1. S.B. Smith, L. Finzi, C. Bustamante, Science **258**, 1122 (1992).
2. T.R. Strick, J.-F. Allemand, D. Bensimon, A. Bensimon, V. Croquette, Science **271**, 1835 (1996).
3. T.R. Strick, J.-F. Allemand, D. Bensimon, V. Croquette, Biophys. J. **74**, 2016 (1998).
4. M. Doi, S.F. Edwards, *Theory of Polymer Dynamics* (Clarendon Press, Oxford, 1986).
5. O. Kratky, G. Porod, Rec. Trav. Chim. **68**, 1106 (1949).
6. N. Saito, K. Takahashi, Y. Yunoki, J. Phys. Soc. Jpn **22**, 219 (1967).
7. K.F. Freed, J. Chem. Phys. **54**, 1453 (1971).
8. M. Fixman, J. Kovac, J. Chem. Phys. **58**, 1564 (1973).
9. D. Thirumalai, B.Y. Ha, in *Theoretical and Mathematical Models in polymer research*, edited by A. Grosberg (Academic Press, Orlando, 1998), pp. 1–35.
10. I.A. Nyrkova, A.N. Semenov, A.N. Joanny, A.R. Khokhlov, J. Phys. II France **6**, 1411 (1996).
11. G.H.M. van der Heijden, J.M. Thompson, Nonlinear Dynamics **21**, 71 (2000).
12. D.M. Stump, P.J. Watson, W.B. Fraser, J. Biomechanics **33**, 407 (2000).
13. I. Tobias, D. Swigon, B.D. Coleman, Phys. Rev. E **61**, 747 (2000).
14. B. Fain, J. Rudnick, S. Östlund, Phys. Rev. E **55**, 7364 (1997).
15. T.R. Strick, V. Croquette, D. Bensimon, Proc. Natl. Acad. Sci. USA **95**, 10579 (1998).
16. J.F. Marko, Phys. Rev. E **55**, 1758 (1997).
17. J.F. Marko, E.D. Siggia, Phys. Rev. E **52**, 2912 (1995).
18. C. Bouchiat, M. Mezard, Eur. Phys. J. E **2**, 377 (2000).
19. F.B. Fuller, Proc. Natl. Acad. Sci. USA **75**, 3557 (1978).
20. J.F. Marko, E.D. Siggia, Macromolecules **27**, 981 (1994).
21. R.D. Kamien, T.C. Lubensky, P. Nelson, C. O'Hern, Europhys. Lett. **38**, 237 (1997).
22. A.C. Maggs, J. Chem. Phys. **114**, 5888 (2001).
23. G. Calugareanu, Czech. Math. J. **11**, 588 (1961).
24. J.H. White, Am. J. Math. **11**, 693 (1969).